

# Analysis of Smoke Composition and Toxicity from Lithium-ion Battery Failure Using Real-Time FTIR Spectroscopy

## Industry/Application

Fire Science, LiB R&D / failure analysis

## Products used

Antaris IGS, 2 m gas cell, Heated Valve Drawer (HVD), ModGas System

## Goals

Demonstrate analysis of vapors generated during LiB failure by FTIR and unique benefits of real-time analysis of vapors.

## Key Analytes

Acid vapors (hydrogen fluoride, hydrogen chloride), carbon monoxide, carbon dioxide, electrolyte vapors (e.g. dimethyl carbonate, diethyl carbonate, ethyl methyl carbonate, etc.), light hydrocarbons/olefins (methane, ethylene, propylene).

## Key Benefits

FTIR spectroscopy provides a balance of speed, specificity, and sensitivity, which is useful for real-time quantitation of vapor concentrations for smoke toxicity testing. The ModGas system has been designed for rapid and simplified integration to support testing per EN 45545-2, EN 17084, and ISO 19702 methods. This document explores the application of the technique to quantitation of gases emitted by failing lithium-ion batteries, which can enhance battery safety and materials development.

## Introduction

Lithium-ion batteries (LiB) have become ubiquitous as a means of energy storage due to their long lifespan, light weight, high energy density, and fast charging speed, among other desirable characteristics. Such properties are advantageous for myriad end uses; these batteries can be found in everyday products such as consumer electronic devices and vehicles, and even in large-scale applications such as grid energy storage. Demand for greater storage capacity and pack voltage has driven advancements in cell design and materials research, as these improvements increase battery run time and reliability, ultimately enhancing the end-user experience. However, these advancements are not without risk, as the lithium compounds which enable these batteries are highly reactive.

Lithium-ion batteries can overheat, catch fire, or explode if charged, stored, or used incorrectly.<sup>1,2</sup> News reports and product recalls have brought awareness to the risks posed by LiB's, ranging from property damage to personal injury and even death.<sup>3,4,5,6,7,8</sup> High current flow during charge or discharge processes can cause cells to heat rapidly, which in turn causes electrolyte solvents to vaporize or decompose and potentially rupture the case. As the battery ages, lithium will fail to re-incorporate into the anode material and instead deposit in branch-like structures known as "dendrites."<sup>9</sup> These dendrite structures pose several hazards in LiB's, as they can potentially bridge anode and cathode layers, causing an electrical short, or they could cause mechanical damage from within the cell by puncturing the separator. Lithium-ion battery failure can also occur if the cell is exposed to heat from external sources, such as motors or other batteries. Puncture or other physical damage to the cell can cause catastrophic failure of the cell as well, as this exposes the reactive materials within the cell to air and moisture.

Figure 1 is a schematic of the components of a typical LiB, consisting of an anode (the negative terminal), a separator, and a cathode (the positive terminal). A solvent is added to facilitate the movement of ions, while the separator (typically a polymer film such as polyethylene or polypropylene) prevents contact between the electrodes—a scenario which would cause an electrical short within the battery and lead to heating of the cell, potentially to the point of failure. Other components and materials may be present in the cell, depending on the design of the battery, including polymer gaskets and insulators.

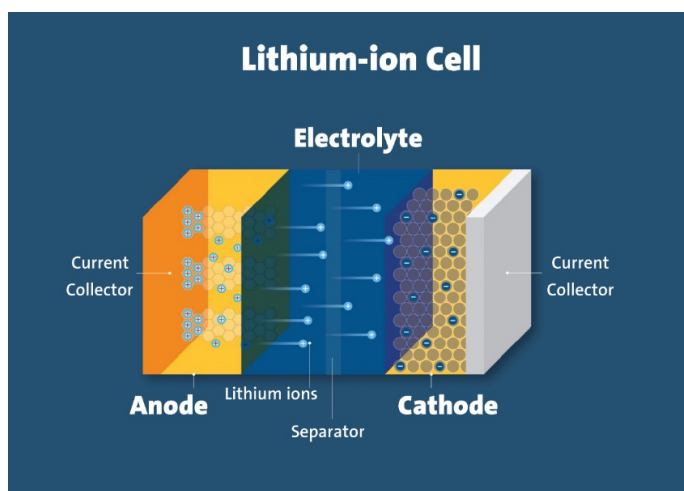


Figure 1. A schematic showing key components of a LiB cell, obtained from BATSTRUCT.

Hazards of LiB failure are not limited to heat and flame, but also include chemical exposure and toxicity of fumes emitted by a ruptured cell. Many of the compounds found in LiB's are known to be toxic or harmful, but the chemistry of decomposition and combustion are quite complex and produce a greater variety of byproducts. For example, lithium hexafluorophosphate can decompose on exposure to heat, producing phosphorus pentafluoride and lithium fluoride (Equation 1 below). Phosphorus pentafluoride and lithium hexafluorophosphate will both readily react with moisture to generate hydrogen fluoride, a highly toxic and corrosive gas<sup>11</sup> (Equations 2 and 3 below).



Equation 1.



Equation 2.



Equation 3.

During thermal runaway processes, other reactions occur which involve typical solvents, such as ethyl carbonate, propyl carbonate, and dimethyl carbonate, and lithium, shown below in Equations 4-7.<sup>12</sup>



Equation 4.



Equation 5.



Equation 6.



Equation 7.

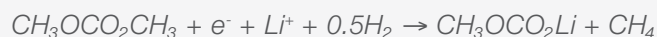
These reactions are exothermic, thus the three components required for fire (heat/ignition source, fuel, and oxygen) drive the thermal runaway process. Research has been devoted to mitigation of such reactions through selection of other more inert electrolyte chemistries, with mixed results thus far from both safety and performance standpoints.<sup>13</sup> Electrochemical reactions can also lead to thermal runaway, involving the electrolyte, lithium ions, and hydrogen. Some examples of such reactions are shown in Equations 8-10.<sup>12</sup>



Equation 8.



Equation 9.



Equation 10.

Such reactions often occur when a cell is charged to levels exceeding the design voltage, a phenomenon known as "overcharging." In all these reactions (Equations 1-10), the liberation of gases will build pressure within the LiB cell and increase the risk of rupture, potentially expelling reactive and harmful compounds.

Considering the nature of these reactions, research efforts have been focused on the efficacy of retardants or encapsulants added to the LiB cells, and their ability to reduce flammability of vented gas.<sup>14,15,16</sup> Incorporation of such materials into the electrolyte and/or separator can affect the electrical characteristics and performance of the cell, but it is also worth noting that these materials can contribute to toxicity of emitted smoke.

Solid-state batteries (SSB's) have garnered much attention for perceived inherent safety through designs which reduce or eliminate the need of liquid electrolyte, yet research suggests these batteries can be more prone to internal short-circuits and accelerated temperature rises.<sup>17</sup> Gases generated by failure of these battery chemistries still pose a risk of toxicity, as the elevated heat can combust the case material or other materials within the battery such as polymers (used as a matrix for the solid electrolyte) or sulfides (used as the solid electrolyte). As such, it is critical for failure testing to be carried out in parallel with battery materials research.

### Comparison of Analytical Techniques

Various analytical techniques have been employed to increase understanding of vapor composition during thermal runaway events in LiB's. These techniques include gas chromatography with mass spectrometry detection (GCMS); Fourier transform infrared (FTIR) spectroscopy; non-dispersive infrared sensors (NDIR); paramagnetic analyzers (PA); and gas-washing bottles.<sup>18</sup> Paramagnetic analyzers (PA) are only sensitive to gases with a high magnetic susceptibility, limiting their typical use to detection of oxygen. The GCMS technology benefits from high sensitivity, while also providing a more-detailed compositional breakdown of chemical species, but only a limited number of samples may be analyzed during a battery test because the sampled material must first be separated in the chromatography column before detection. Gas-washing bottles provide a means to measure the total quantity of a gas or category of compounds captured within a range of time, but this approach is also dependent on solubility of the target compound(s) in the wash solution and requires additional analysis. Little to no temporal resolution is available with this approach—that is, no detail is provided as to the timing or rate of release of a compound over the course of the test.

Spectroscopic techniques like NDIR can provide stable measurement of gases with higher temporal resolution, but the sensors are limited to one or a few gases, depending on the number of filters fitted to the instrument. These sensors are often configured to measure a narrow spectral band for each analyte, but this limits flexibility. It also does not provide any information relating to interference from species with broader overlapping spectral absorbances, which is typical of larger molecular species such as electrolytes and C3+ hydrocarbons. Measurements from NDIR analyzers are also not useful for interpretive purposes, such as functional group identification or identification of unknown species. Figure 2 summarizes strengths of these different techniques.

		Technique				
		PA	GWB	GC-MS	NDIR	FT-IR
Characteristics	Detection of oxygen	+				
	Sensitive detection	+	+	++	+	+
	Compositional detail			++		+
	Real-time analysis	++			++	++

**Figure 2. Comparison of strengths of various analytical techniques used to analyze composition of smoke emitted from LiB cells. Analytical techniques such as paramagnetic analyzers (PA), gas washing bottles (GWB), gas chromatography with mass spectrometry detection (GC-MS), non-dispersive infrared sensors (NDIR), and Fourier Transform Infrared (FTIR) spectrometers are typically used for these analyses.**

Figure 3 shows infrared spectra of carbon monoxide (CO), hydrogen chloride (HCl), hydrogen fluoride (HF), and sulfur dioxide (SO<sub>2</sub>). These toxic gases are commonly released upon failure of LiB's. The relative simplicity of their infrared spectral features is a result of the structure of each molecule—CO, HCl, and HF are diatomic molecules with a linear geometry, so the spectral features are those of a stretching vibration of one bond; SO<sub>2</sub> is triatomic with a bent (*v*-shaped) geometry, resulting in spectral features associated with antisymmetric stretching (those near 1360 cm<sup>-1</sup>), symmetric stretching (near 1150 cm<sup>-1</sup>), and bending of the molecule (near 600 cm<sup>-1</sup>, outside the measured range). The trend of increasing molecular complexity causing increased spectral complexity is especially apparent when examining the spectra of some of the hydrocarbons emitted upon failure of LiB's.

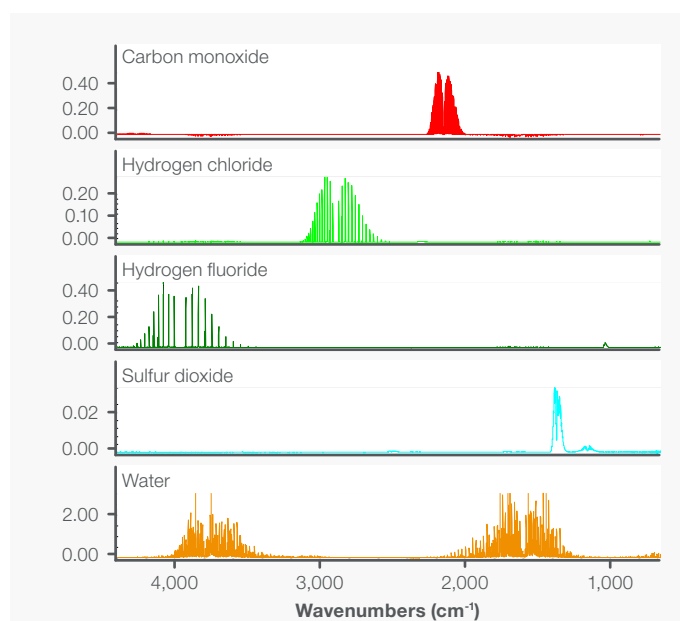


**Figure 3. Infrared spectra of carbon monoxide, hydrogen chloride, hydrogen fluoride, and sulfur dioxide. These are examples of toxic gases commonly released on failure of LiB cells. Note the high overlap of spectral features between water vapor and hydrogen fluoride and sulfur dioxide, which can be mitigated by measurement at 0.5 cm<sup>-1</sup> spectral resolution.**

Figure 4 shows the infrared spectra of methane (CH<sub>4</sub>), ethylene (C<sub>2</sub>H<sub>4</sub>), propylene (C<sub>3</sub>H<sub>6</sub>), dimethyl carbonate (C<sub>3</sub>H<sub>6</sub>O<sub>3</sub>), and ethyl methyl carbonate (C<sub>4</sub>H<sub>8</sub>O<sub>3</sub>). Note the drastic change in appearance and complexity of the infrared spectral features moving from top (methane) to bottom (ethyl methyl carbonate) in the figure. The spectrum of methane contains a repeating set of sharp bands because of the relative simplicity of the molecular structure—only one type of bond (C–H) is present in the molecule. As the structure of the molecules becomes more complex, more types of bonds are present. For example, ethyl methyl carbonate consists of a total of fifteen atoms and contains bonds between carbon and hydrogen (C–H), carbon and carbon (C–C), and carbon and oxygen in two forms: a carbon-oxygen single bond (C–O), and a carbon-oxygen double bond (C=O). With this level of complexity, so many vibrational states are possible that the spectrum starts to resemble that of a condensed-phase (e.g. liquid) spectrum. Any one state and conformation of the molecule would produce a sharp band, but there are so many of these bands, so closely spaced, that the spectrum takes on a “smoother” appearance. These broad absorbances result in greater overlap between the spectral features of different species, a challenge which will be discussed later in greater detail.

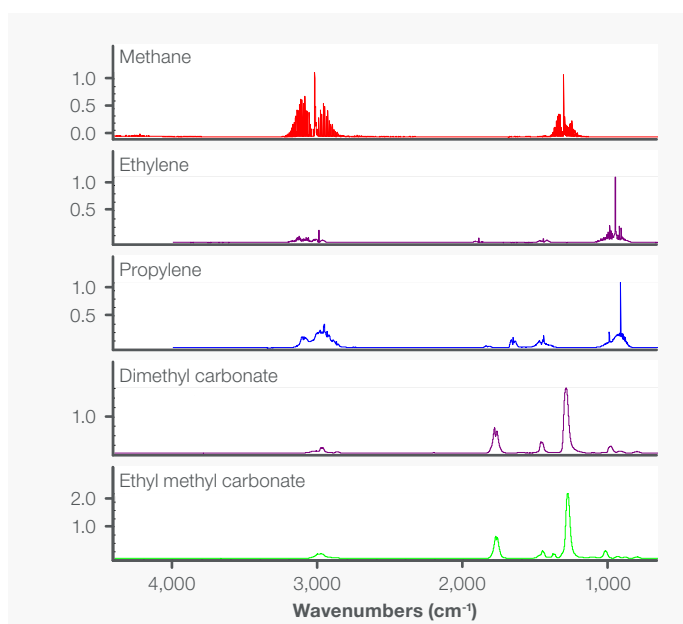


Figure 4. Infrared spectra of methane, ethylene, propylene, dimethyl carbonate, and ethyl methyl carbonate. These are all hydrocarbons whose vapors are typically released upon failure of LiB cells.

For these reasons, FTIR spectroscopy is a preferred analytical technique for analysis of constituents in smoke generated by LiB failure, as it can provide rapid measurement of a broad range of compounds. The speed of the measurement enables analysis of species which are transient, delivering compositional detail with rapidly changing chemistries emanating from the battery. Measurement of a broad spectral range allows methods to be adapted to changing electrolytes and retardants, providing researchers and manufacturers with critical insights into the properties and safety of their proprietary battery materials.

### Enhancing Understanding of Failures and Smoke Toxicity

In addition to battery chemistry and materials, research into LiB failure mechanisms has also revealed a connection between the state of charge (SOC) of the battery and the rate of release of toxic fumes, such as hydrogen fluoride (HF), on failure of the cell when exposed to high heat from a gas burner.<sup>19</sup> Researchers found that HF was released early and at higher rates when the battery was fully charged, while HF was released at a lower rate, with greater delay, at decreased charge levels. Spectra were acquired once every 12 seconds to quantitate the generated vapors, a rate of analysis not attainable with other analytical techniques. Figure 5 (obtained from *Sci Rep* 7, 10018 (2017); see reference 19) shows a plot of the measured HF vapor concentration as a function of time for batteries at five different charge states.

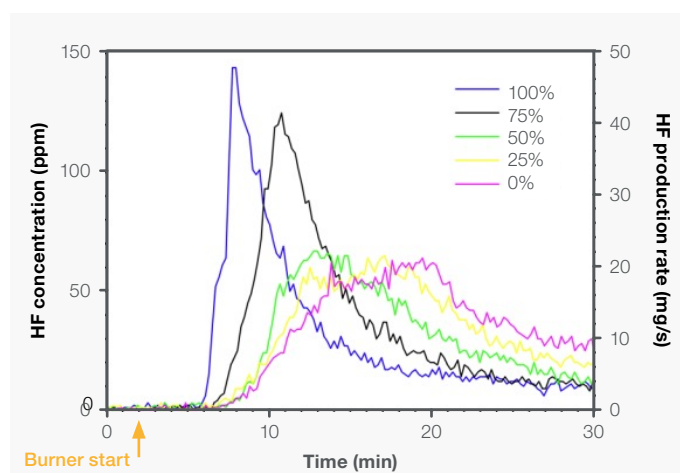


Figure 5. Concentration of HF vapor measured during LiB thermal runaway with cells at different charge states, published in *Sci Rep* 7, 10018 (2017) (see reference 19).

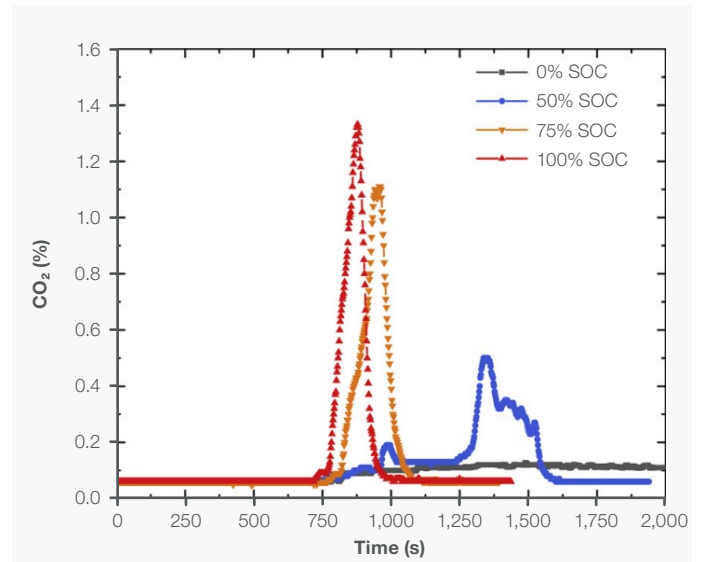
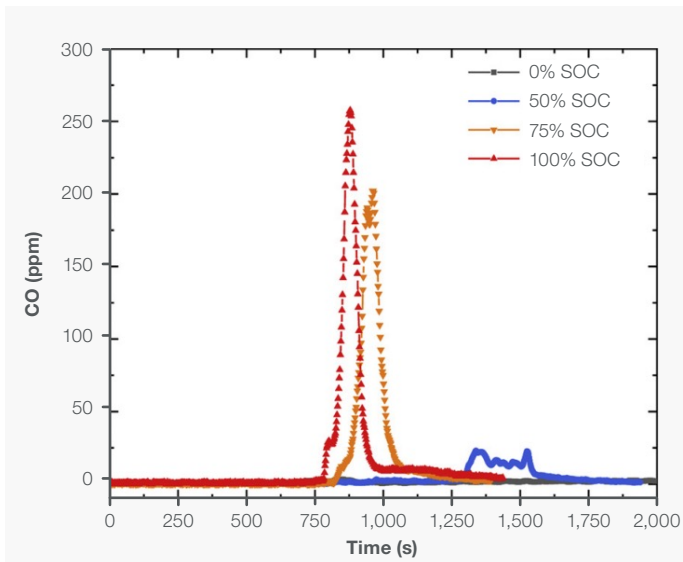


Figure 6. Concentrations of CO and CO<sub>2</sub> measured as a function of test time during thermal runaway of a large format LiB pack, published in *Journal of Hazardous Materials*, Volume 381, 2020 (see reference 20).

Research has revealed a similar dependency between SOC and other gases. Another research group tested large-format LiB's (68 Ah lithium iron phosphate pouches) exposed to heat using electric heaters, allowing straightforward interpretation of FTIR measurements of combustion byproducts such as carbon monoxide (CO) and carbon dioxide (CO<sub>2</sub>).<sup>20</sup> Figure 6 shows the concentration of these gases as a function of test time. Other gases analyzed, including HF, sulfur dioxide (SO<sub>2</sub>), nitric oxide (NO), and nitrogen dioxide (NO<sub>2</sub>), followed similar time-concentration trends, as well as a similar dependence between onset of detection, magnitude of concentration, and SOC; that is, the evolution of vapors was delayed, and the rate of evolution was slower, at lower states of charge.

FTIR spectroscopy has also been employed for the study of gases released from LiB's during failure caused by overcharging.<sup>21</sup> In this study, the authors note the difference in cell temperature between overcharge testing and thermal abuse testing. This different failure mode leads to different proportions of gases released, of which the electrolytes ethyl methyl carbonate (EMC) and dimethyl carbonate (DMC) are major constituents. Lower temperatures outside the cell under testing can prevent combustion, which would otherwise cause conversion of the electrolyte species to compounds like CO, CO<sub>2</sub>, and H<sub>2</sub>O. In comparison to thermal abuse testing, this also results in delayed detection of HF vapor, as the fluorinated components of the cell are not rapidly exposed to moisture. Figure 7 shows the concentration trends of vapors measured in this study.

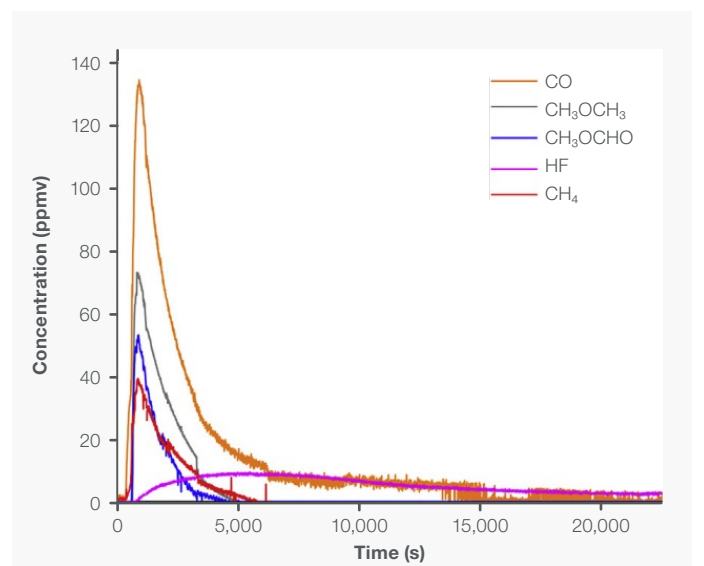
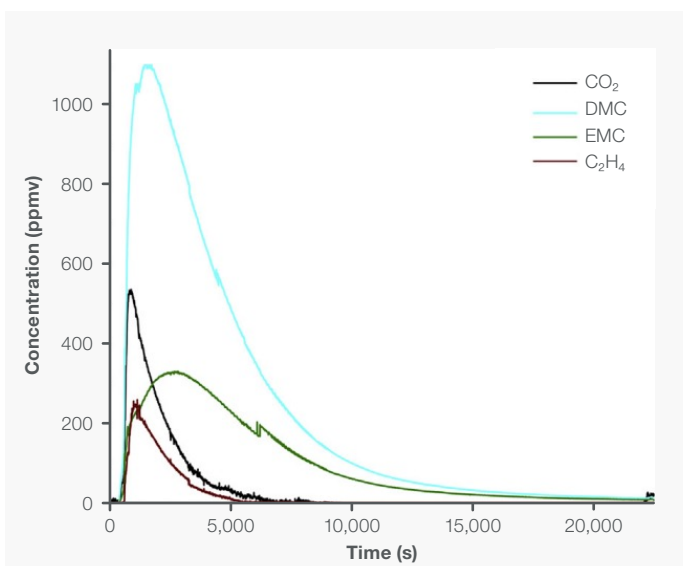


Figure 7. Concentrations of CO<sub>2</sub>, DMC, EMC, and ethylene (C<sub>2</sub>H<sub>4</sub>) at left, and CO, dimethyl ether (CH<sub>3</sub>OCH<sub>3</sub>), methyl formate (CH<sub>3</sub>OCHO), HF, and methane (CH<sub>4</sub>) at right. Vapors were released on overcharge testing of a LiB. Originally published in *Journal of Power Sources*, Volume 389, 2018 (see reference 21).



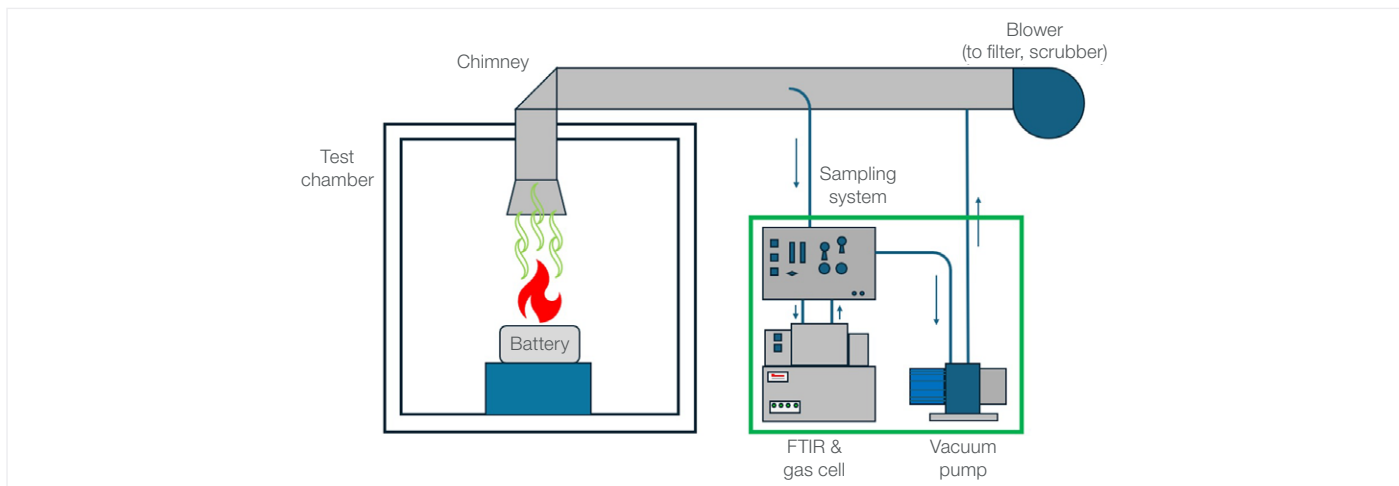


Figure 8. A diagram (top) showing common components of a battery test setup with the HVD and Antaris™ IGS gas analysis system (shown in Figure 9 below).

### The Antaris IGS FTIR Gas Analyzer – Power and Flexibility

Thermo Fisher Scientific has developed a complete FTIR measurement system to support smoke toxicity tests as described in standard smoke toxicity protocols such as EN17084, EN 45545-2, and ISO 19702. This system is comprised of the Thermo Scientific™ Antaris™ IGS Gas Analyzer System with a rack-mounted Heated Valve Drawer (HVD) and vacuum pump, referred to collectively as the “ModGas System.” Features of this system include the following:

- High-sensitivity quantitation of many compounds in a single measurement
- High-resolution ( $0.5\text{ cm}^{-1}$ ) measurements, permitting quantitative analysis where spectral bands would otherwise be overlapped
- Optional integrated pressure and temperature measurement for automated adjustment of reported concentration values to increase accuracy
- Certified Fire Science analysis method, validated to primary calibration standards
- Direct online sampling for real-time, second-by-second analysis
- Ability to re-analyze stored data and add species for customized testing and research
- Ability to search spectra of unknown species against spectral libraries using the Thermo Scientific™ OMNIC™ Software

The components of the ModGas System are essential to accurate measurement of gases evolved during smoke toxicity testing, as they also 1) prevent loss of reactive gases to surfaces with low chemical resistance, 2) prevent loss of condensing gases to cold surfaces, and 3) reduce interference resulting from sample carryover. Additional details are available upon request to Thermo Fisher Scientific.

An experimental setup such as the configuration shown in Figure 8 is typical of battery failure analysis and smoke toxicity tests. The battery cell or pack is placed in a chamber or room beneath a vent draw point or “chimney.” Gases released during testing are pulled by a blower through the chimney, and a portion of these gases are drawn via a probe from the chimney to the HVD and the Antaris IGS using a vacuum pump in a “pull” configuration. Sample gases are thus measured in the gas cell at pressures slightly below ambient pressure ( $\sim 760\text{ Torr}$ ); as such, Thermo Fisher Scientific calibrates the FTIR instruments at a pressure of 650 Torr. Once the vapors have flowed through the gas cell, they flow back to the HVD and exit via a vent connection. The HVD also provides a convenient means to introduce other gases to the Antaris IGS through nitrogen and span gas connections. These can be used for periodic checks of the accuracy of the measurements, or to introduce calibration gases to be used in new methods. Flow rates and sample gas pressure can also be adjusted with the HVD to ensure consistency in test protocols.



Figure 9. The Thermo Scientific Antaris IGS Gas Analyzer.

Spectral acquisition is controlled with the OMNIC Series software module, which allows users to visualize spectral data and concentration trends in real time as time-resolved experiments are conducted. To begin, users will set spectral measurement parameters in the Collect menu. Once measurement parameters have been defined, the Series menu is used to specify the duration of the experiment, the time segments during which data may be saved or discarded, and profiles displayed during spectral acquisition. Profiles allow users to calculate and view concentration trends in real time. Profiles may consist of quantitative methods assembled in TQ Analyst; basic spectral parameters such as peak height, position, area, noise, etc. configured as “Measurement Only” methods in TQ Analyst; or profiles such as a Gram-Schmidt reconstruction. These parameters can be saved in an experiment file, which allows users to quickly and easily recall experimental parameters which are regularly used in their laboratory. Figure 10 shows an example of a Series experiment. At top are concentration profiles (in ppm) for a range of gases, including methane (CH<sub>4</sub>), nitric oxide (NO), and carbon monoxide (CO). Each data point along these curves has a corresponding infrared spectrum, shown in the bottom section of the window.

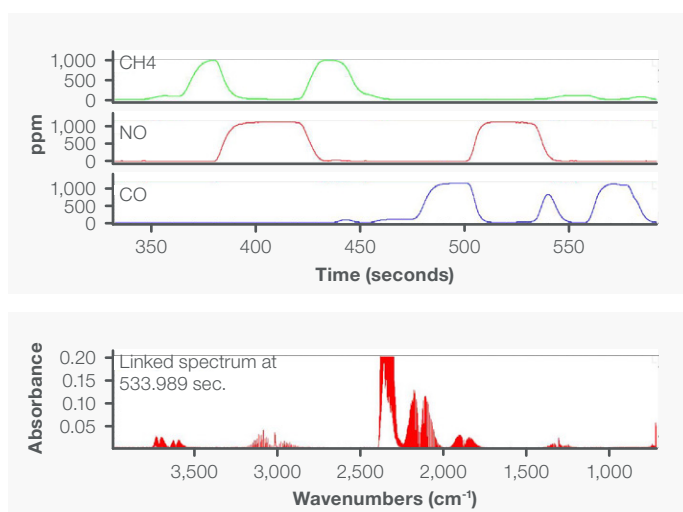


**Figure 10. Example series profiles of a dynamic mixture of gases. The top section displays the measured concentrations of the gases, and the bottom section displays the infrared spectrum collected at the selected time point on the profile.**

The Antaris IGS spectrometer can also be controlled by the RESULT software, acquiring spectral data using the Sequence function. This software package was designed with industrial users in mind, as it allows assembly of “workflows,” which are a sort of analytical recipe. During operation of the workflows, measurement parameters are not displayed to the user, thus reducing the possibility of error in experimental configuration. Additionally, the software includes capabilities for reception and transmission of signals via popular industrial protocols such as Modbus or OPC DA/UA, allowing seamless integration of the spectrometer with automation systems.

Quantitative methods are constructed and maintained in the TQ Analyst software, allowing users to adapt their research to emerging battery material technologies. For example, as demand increases for higher cell voltages, research has focused on development of electrolyte solvent chemistries which do not break down at such voltages. This has led researchers to test fluorinated carbonates,<sup>22</sup> and a variety of other electrolyte chemistries, to enhance the performance and/or safety of the cells.<sup>23</sup> User-customizable methods allow researchers to adapt their analytical system to measure novel materials and battery chemistries, keeping them at the cutting edge of technological developments.

Selection of appropriate spectral resolution is critical for accurate quantitation of gases in mixtures, which is the rationale behind the guidance in EN 17084. Figure 11 shows spectra of water vapor and nitric oxide at 4 cm<sup>-1</sup> resolution and 0.5 cm<sup>-1</sup> resolution. At broader resolution, the spectral bands of the two vapors overlap, reducing the accuracy of quantitative measurements of nitric oxide. At 0.5 cm<sup>-1</sup> resolution, the overlap of the two is practically eliminated, making the highlighted spectral region useful for quantitation of nitric oxide. Thermo Scientific OMNIC software allows users to collect spectra at narrow spectral resolution and re-process the data to broader resolutions. With this capability, researchers can rapidly evaluate the impact of spectral resolution on their methods without manually re-collecting data, therefore streamlining method optimization.

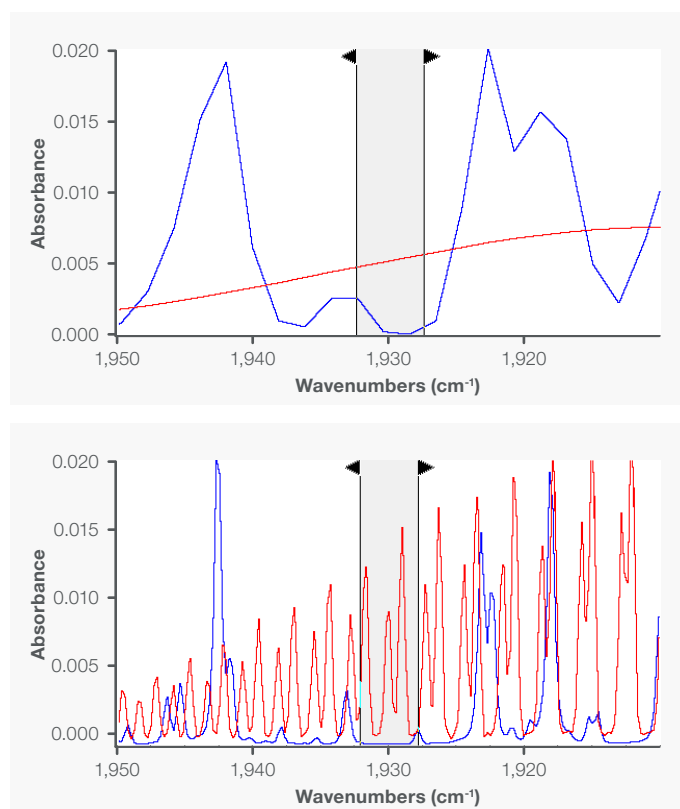


**Figure 11. Overlaid infrared spectra of water vapor (in blue) and nitric oxide (in red) at 4 cm<sup>-1</sup> resolution (top), and 0.5 cm<sup>-1</sup> resolution (bottom). Note the overlap between the spectral features when data is collected at 4 cm<sup>-1</sup> resolution. The cursors highlight a spectral region useful for quantitation of NO, but only at 0.5 cm<sup>-1</sup> resolution.**

Gas calibrations are constructed with spectra of vapors collected at multiple concentrations. To create a new method, or add a new gas to an existing method, spectra are collected with the gas, then added to the list of standards. Corresponding concentration values are added to the table with the standards, and one or more spectral ranges are specified for use in quantitation of the compound. Ideally, the selected range will contain only the spectral features of the analyte, minimizing interference by other compounds, as in the example of nitric oxide shown above. In cases where this is not possible, Thermo Fisher Scientific's unique implementation of CLS in the TQ Analyst software allows users to identify compounds as interferences, which will subtract spectral features of interferences from the analyte spectral region when quantifying the species, thereby increasing the accuracy of measurement of species with overlapping spectral features and mitigating interference from non-analyte species. Spectral ranges which are optimal for quantitative analysis can be designated as analytical regions, allowing the user to ensure the model incorporates the best spectral bands for sensitive detection and quantitation of the analytes.

While many different algorithms are employed for quantitative analysis with infrared spectral data, classical least squares (CLS) has long been the preferred algorithm for analysis of gas-phase species in complex mixtures. This algorithm utilizes a range of spectral data points for quantitation, assuming a summative relationship between components in mixtures. Calculation of concentration using a range of data points benefits from a sort of averaging effect; the analyte's calculated concentration is not so heavily influenced by spectral noise at a single frequency, and noise will vary randomly across multiple points such that the overall contribution is reduced when the data points are used in concert. The most accurate methods will contain measured spectra of any vapor constituents which absorb infrared light in the frequency range(s) of any analytes.

Other approaches, such as peak height calibrations, will be more sensitive to spectral noise, thus providing diminished limits of detection. Peak area approaches will gain some of the averaging benefit, but quantitation across larger ranges with spectral overlap proves tedious, as calculated areas would need to account for contribution from interfering species. More sophisticated algorithms such as partial least squares (PLS) are well-suited to quantitative problems where spectral features of species are overlapped; PLS also reduces the impact of spectral noise, but this algorithm brings an increased burden of calibration. Typically, many samples must be prepared and tested to calibrate a robust PLS model, as the tested samples must have minimal covariance in the concentrations of the species for development of an accurate method.

Additionally, while CLS allows users to assemble methods with spectra of individual pure analytes, PLS is calibrated with spectra of representative mixtures. This unfortunately means that expansion of a method to include a new gas will require preparation and spectral acquisition with a whole new set of gas mixtures which now include the new analyte along with all other interfering species.

Quantitative methods for vapor-phase species often incorporate additional corrections for non-linearity in the calibration curve. The non-linear relationship between the concentration and the magnitude of absorbance can have several causes. While  $0.5\text{ cm}^{-1}$  resolution is sufficient to resolve spectral bands to a level where closely spaced spectral bands of species like HF, H<sub>2</sub>O, and NO can be distinguished with little overlap, this resolution is still broader than the true line width of some of the small linear molecules routinely analyzed in smoke toxicity analyses. However, if the true line width of the band increases significantly across the concentration range of the method, the increase in absorption with increased concentration will be spread across a broader range of frequencies, reducing the absorbance-per-concentration slope of the calibration curve. The same is true for gases where collisional broadening increases significantly across the calibration curve; polar gases are particularly likely to do this, as their collisional cross-section is greater than those of other gases. Lastly, the detector in the FTIR may not provide a linear response. Mercury cadmium telluride (MCT) detectors are prized for their sensitivity, which can provide low limits of detection and high scan speeds, but these detectors will often deliver a non-linear response to otherwise-linear changes in absorbance. The TQ Analyst software package allows users to fit the calibration points with quadratic and higher order polynomial curves to accurately account for the complex changes which can occur across the calibration range.

One other scenario is worth mentioning: When the concentration of the analyte is high enough that a portion of the original analytical region is "saturated", meaning there is little or no measurable light in the spectral range, random noise will be the dominant contributor to the measured signal in these regions. As such, there is no benefit in attempting to use these frequencies for quantitation. Instead, the analyte is often quantified using a different spectral region, one where the magnitude of absorbance is within an acceptable range. This is a common best practice for quantitative measurement of gaseous species with FTIR, wherein the strongest spectral bands are used for quantitation at low concentrations, providing the best possible sensitivity and therefore lowest limits of detection, while weaker spectral bands are used to quantitate the analyte at very high concentrations to avoid saturation. This practice expands the calibration range of the instrument.



## Summary

Research has highlighted the need for smoke toxicity testing with lithium-ion batteries due to the reactive and harmful materials used to construct the cells. The rate and overall quantity of toxic gases released from the cell is dependent on the chemistry employed in the battery, as well as the state of charge, and these characteristics will no doubt continue to evolve as new battery chemistries are developed.

The Antaris IGS and ModGas sampling interface provide a powerful and flexible system which enables researchers to better understand battery failure mechanisms and the toxicity of the vapors generated during battery failure. Spectral data can be reprocessed and can be searched against library databases to aid identification of unknown species. Through this approach, researchers can update and adapt their methods to accommodate emerging material technologies, as well as supporting the development of novel battery materials.

## References

1. "Lithium-Ion Battery Safety," n.d. <https://www.nfpa.org/education-and-research/home-fire-safety/lithium-ion-batteries>.
2. Chen, Yuqing, Yuqiong Kang, Yun Zhao, Li Wang, Jilei Liu, Yanxi Li, Zheng Liang, et al. "A Review of Lithium-ion Battery Safety Concerns: The Issues, Strategies, and Testing Standards." *Journal of Energy Chemistry* 59 (November 3, 2020): 83–99. <https://doi.org/10.1016/j.jechem.2020.10.017>.
3. Gibson, Kate. "Baseus Power Banks Recalled After Dozens of Fires, 13 Burn Injuries." CBS News, June 29, 2024. <https://www.cbsnews.com/news/lithium-ion-battery-fires-product-recall-cpsc/>.
4. United States Consumer Product Safety Commission, "Snap Recalls Lithium-Ion Battery Sold for Pixy Flying Cameras Due to Fire Hazard," accessed January 6, 2025, <https://www.cpsc.gov/Recalls/2024/Snap-Recalls-Lithium-Ion-Battery-Sold-for-Pixy-Flying-Cameras-Due-to-Fire-Hazard>
5. United States Consumer Product Safety Commission, "HALO 1000 Portable Power Stations Recalled Due to Serious Fire and Burn Hazards; One Death Reported; Imported by ZAGG; Sold by ACG, QVC and ZAGG," accessed January 6, 2025, <https://www.cpsc.gov/Recalls/2024/HALO-1000-Portable-Power-Stations-Recalled-Due-to-Serious-Fire-and-Burn-Hazards-One-Death-Reported-Imported-by-ZAGG-Sold-by-ACG-QVC-and-ZAGG>
6. Division of Homeland Security and Emergency Services. "LG Energy Solution Michigan Recalls Home Energy Storage Batteries Due to Fire Hazard," n.d. <https://www.dhss.ny.gov/lg-energy-solution-michigan-recalls-home-energy-storage-batteries-due-fire-hazard>.
7. L. Ly and S. Murphy Kelly, "Fire that Killed 4 at NYC E-Bike Store was Caused by Lithium Ion Batteries, Fire Commissioner Says," Cable News Network, accessed January 6, 2025, <https://www.cnn.com/2023/06/20/us/nyc-ebike-store-fire-lithium-ion-batteries/index.html>
8. A. Moshtaghian, I. Kaufman-Geballe and S. Beech, "Scooter Lithium Battery Investigated as Cause of 5-Alarm Bronx Blaze, Fire Department Says," Cable News Network, accessed January 6, 2025, <https://www.cnn.com/2023/03/05/us/nyc-bronx-lithium-battery-fire/index.html>
9. Agubra, Victor, and Jeffrey Fergus. "Lithium Ion Battery Anode Aging Mechanisms." *Materials* 6, no. 4 (March 27, 2013): 1310–25. <https://doi.org/10.3390/ma6041310>.
10. "What Are Lithium-Ion Batteries? | UL Research Institutes," n.d. <https://ul.org/research/electrochemical-safety/getting-started-electrochemical-safety/what-are-lithium-ion>.
11. Swiderska-Mocek, A., P. Jakobczyk, E. Rudnicka, and A. Lewandowski. "Flammability Parameters of Lithium-ion Battery Electrolytes." *Journal of Molecular Liquids* 318 (August 5, 2020): 113986. <https://doi.org/10.1016/j.molliq.2020.113986>.
12. Liu, Kai, Yayuan Liu, Dingchang Lin, Allen Pei, and Yi Cui. "Materials for Lithium-ion Battery Safety." *Science Advances* 4, no. 6 (June 1, 2018). <https://doi.org/10.1126/sciadv.aas9820>.
13. Roth, E. P., and C. J. Orendorff. "How Electrolytes Influence Battery Safety." *The Electrochemical Society Interface* 21, no. 2 (January 1, 2012): 45–49. <https://doi.org/10.1149/2.f04122if>.
14. Liu, Kai, Wei Liu, Yongcai Qiu, Biao Kong, Yongming Sun, Zheng Chen, Denys Zhuo, Dingchang Lin, and Yi Cui. "Electrospun Core-shell Microfiber Separator With Thermal-triggered Flame-retardant Properties for Lithium-ion Batteries." *Science Advances* 3, no. 1 (January 6, 2017). <https://doi.org/10.1126/sciadv.1601978>.
15. Hyung, Yoo E, Donald R Vissers, and Khalil Amine. "Flame-retardant Additives for Lithium-ion Batteries." *Journal of Power Sources* 119–121 (April 7, 2003): 383–87. [https://doi.org/10.1016/s0378-7753\(03\)00225-8](https://doi.org/10.1016/s0378-7753(03)00225-8).
16. Doughty, Daniel H., E. Peter Roth, Chris C. Crafts, G. Nagasubramanian, Gary Henriksen, and Khalil Amine. "Effects of Additives on Thermal Stability of Li Ion Cells." *Journal of Power Sources* 146, no. 1–2 (June 2, 2005): 116–20. <https://doi.org/10.1016/j.jpowsour.2005.03.170>.
17. Bates, Alex M., Yuliya Preger, Loraine Torres-Castro, Katharine L. Harrison, Stephen J. Harris, and John Hewson. "Are Solid-state Batteries Safer Than Lithium-ion Batteries?" *Joule* 6, no. 4 (March 7, 2022): 742–55. <https://doi.org/10.1016/j.joule.2022.02.007>.
18. Rappalber, Tim, Nawar Yusfi, Simone Krüger, Sarah-Katharina Hahn, Tim-Patrick Fellingner, Jonas Krug Von Nidda, and Rico Tschirschwitz. "Meta-analysis of Heat Release and Smoke Gas Emission During Thermal Runaway of Lithium-ion Batteries." *Journal of Energy Storage* 60 (January 8, 2023): 106579. <https://doi.org/10.1016/j.est.2022.106579>.
19. Larsson, Fredrik, Petra Andersson, Per Blomqvist, and Bengt-Erik Mellander. "Toxic Fluoride Gas Emissions From Lithium-ion Battery Fires." *Scientific Reports* 7, no. 1 (August 24, 2017). <https://doi.org/10.1038/s41598-017-09784-z>.
20. Peng, Yang, Lizhong Yang, Xiaoyu Ju, Baisheng Liao, Kai Ye, Lun Li, Bei Cao, and Yong Ni. "A Comprehensive Investigation on the Thermal and Toxic Hazards of Large Format Lithium-ion Batteries With LiFePO<sub>4</sub> Cathode." *Journal of Hazardous Materials* 381 (July 24, 2019): 120916. <https://doi.org/10.1016/j.jhazmat.2019.120916>.
21. Fernandes, Y., A. Bry, and S. De Persis. "Identification and Quantification of Gases Emitted During Abuse Tests by Overcharge of a Commercial Li-ion Battery." *Journal of Power Sources* 389 (April 11, 2018): 106–19. <https://doi.org/10.1016/j.jpowsour.2018.03.034>.
22. Zhang, Zhengcheng, Libo Hu, Huiming Wu, Wei Weng, Meiten Koh, Paul C. Redfern, Larry A. Curtiss, and Khalil Amine. "Fluorinated Electrolytes for 5 V Lithium-ion Battery Chemistry." *Energy & Environmental Science* 6, no. 6 (January 1, 2013): 1806. <https://doi.org/10.1039/c3ee24414h>.
23. Chawla, Neha, Neelam Bharti, and Shailendra Singh. "Recent Advances in Non-Flammable Electrolytes for Safer Lithium-Ion Batteries." *Batteries* 5, no. 1 (February 1, 2019): 19. <https://doi.org/10.3390/batteries5010019>.

Learn more at [thermofisher.com/ftir](https://thermofisher.com/ftir)

thermo scientific

For research use only. Not for use in diagnostic procedures. For current certifications, visit [thermofisher.com/certifications](https://thermofisher.com/certifications)

© 2025 Thermo Fisher Scientific Inc. All rights reserved. All trademarks are the property of Thermo Fisher Scientific and its subsidiaries unless otherwise specified. MCS-AN1260-EN 01/25